Effect of water uptake on the fracture behavior of low-k organosilicate glass

Xiangyu Guo, Joseph E. Jakes, Samer Banna, Yoshio Nishi, and J. Leon Shohet

Citation: Journal of Vacuum Science & Technology A **32**, 031512 (2014); doi: 10.1116/1.4871680
View online: http://dx.doi.org/10.1116/1.4871680
View Table of Contents: http://scitation.aip.org/content/avs/journal/jvsta/32/3?ver=pdfcov
Published by the AVS: Science & Technology of Materials, Interfaces, and Processing

Articles you may be interested in

The effect of water uptake on the mechanical properties of low-k organosilicate glass
J. Appl. Phys. **114**, 084103 (2013); 10.1063/1.4817917

The effects of vacuum ultraviolet radiation on low-k dielectric films
J. Appl. Phys. **112**, 111101 (2012); 10.1063/1.4751317

Water diffusion and fracture behavior in nanoporous low- k dielectric film stacks
J. Appl. Phys. **106**, 033503 (2009); 10.1063/1.3187931

Fracture of Lowk Dielectric Films and Interfaces
AIP Conf. Proc. **817**, 83 (2006); 10.1063/1.2173535

Nanoscratch evaluation of adhesion and cohesion in SiC/low-k/Si stacked layers
J. Appl. Phys. **95**, 3704 (2004); 10.1063/1.1664025

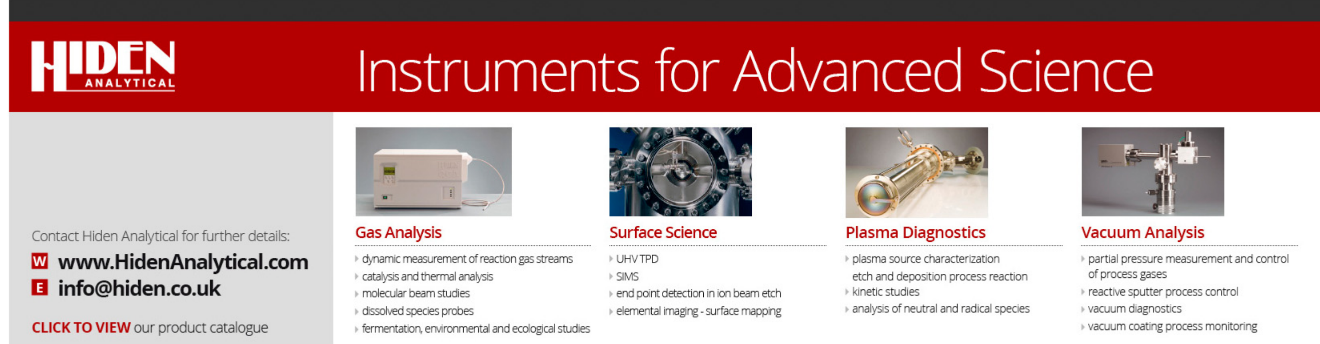

Redistribution subject to AVS license or copyright; see http://scitation.aip.org/termsconditions. Download to IP: 128.104.180.203 On: Mon, 21 Apr 2014 19:50:41

Effect of water uptake on the fracture behavior of low-*k* organosilicate glass

Xiangyu Guo
Plasma Processing and Technology Laboratory and Department of Electrical and Computer Engineering, University of Wisconsin-Madison, Madison, Wisconsin 53706

Joseph E. Jakes
Forest Biopolymer Science and Engineering, USDA Forest Service Forest Products Laboratory, Madison, Wisconsin 53726

Samer Banna
Applied Materials, Sunnyvale, California 94085

Yoshio Nishi
Department of Electrical Engineering, Stanford University, Stanford, California 94305

J. Leon Shohet[a)]
Plasma Processing and Technology Laboratory and Department of Electrical and Computer Engineering, University of Wisconsin-Madison, Madison, Wisconsin 53706

(Received 30 December 2013; accepted 7 April 2014; published 18 April 2014)

Water uptake in porous low-*k* dielectrics has become a significant challenge for both back-end-of-the-line integration and circuit reliability. This work examines the effects of water uptake on the fracture behavior of nanoporous low-*k* organosilicate glass. By using annealing dehydration and humidity conditioning, the roles of different water types and their concentrations are analyzed in detail. For as-deposited SiCOH films, annealing dehydration can enhance the resistance to crack occurrence, and these enhancements can be offset by higher humidity conditioning. It was found that the film-cracking threshold can be lowered by in-diffused water in the film as well as by water at the SiCOH/subtract interface. This occurs because the water decreases the film fracture energy and adhesion energy, respectively. By conditioning at high humidity, the variation of the film cracking threshold agrees well with the behavior of the film hardness and modulus of elasticity as a function of relative humidity. The crack morphologies of low-*k* porous films are also implicitly related to water uptake in the materials. Film cracking thresholds and crack morphologies of UV-cured low-k materials exhibit a weaker dependence on the water uptake, indicating a low degree of hydrophilicity of the SiCOH film after UV curing, which corroborates the previous results. Furthermore, by measuring the surface crack length, the material–fracture toughness can be found. The results demonstrate that neither annealing dehydration nor water uptake have significant effects on fracture toughness of as-deposited SiCOH, while for UV-cured SiCOH, annealing enhances the film-fracture toughness. © *2014 American Vacuum Society*. [http://dx.doi.org/10.1116/1.4871680]

I. INTRODUCTION

Low-*k* porous organosilicate glass (OSG), i.e., porous SiO_2 with the addition of hydrophobic methyl groups (-CH_3) lining the pores, has attracted much attention and are widely accepted due to their enormous potential as an alternative to conventional SiO_2 for intermetal dielectrics.[1–3] However, these originally hydrophobic porous-structured low-*k* dielectrics have been found to become hydrophilic after plasma processing (e.g., photoresist stripping and cleaning).[4] For example, CF_x polymers that are deposited during the etching of low-*k* dielectric films in fluorocarbon plasmas can introduce hydrophilic properties to these films because they are not as hydrophobic as the -CH_3 groups.[5] Additionally, oxygen plasma, usually used to remove organic photoresist polymers, can also remove the original hydrophobic groups (-CH_3) and create some free radical sites (-SiO_2•), resulting in the formation of hydrophilic -SiO_2-OH groups.[6] These hydrophilic groups enable significant amounts of water to be absorbed from humid air following diffusion into the dielectric bulk through interconnected pores,[7] which degrade the film's dielectric properties and worsen reliability.[8] Knowledge of the actual mechanism and influence of various absorbed water components on the mechanical properties of porous low-*k* OSG result in some important implications for fabrication of interconnect structures, such as postprocessing of film/substrate interfaces in dielectric-film stacks.[9] Much work has been done to investigate the moisture absorption and transport mechanisms in porous low-*k* dielectrics and the effects of absorbed water on their *electrical* properties and reliability.[10]

Our previous work has investigated the effects of water uptake on hardness and elastic modulus and showed that for nanoporous low-*k* OSG, film hardness and elastic modulus are intimately linked to the type and concentration of the absorbed water in the dielectric bulk.[11] Dehydration of the in-diffused water, either physisorbed (α-bonded) water or chemisorbed (β-bonded) water,[12] has been found to decrease the film's hardness and elastic modulus.[11] And compared with α-bonded water, β-bonded water has a more significant influence on the dielectric film hardness and modulus.

[a)]Electronic mail: shohet@engr.wisc.edu

Redistribution subject to AVS license or copyright; see http://scitation.aip.org/termsconditions. Download to IP: 128.104.180.203 On: Mon, 21 Apr 2014 19:50:41

Another challenge to successful fabrication of low-*k* films lies in the film's ability to endure various forms of stress corrosion, such as chemical–mechanical polishing and wire-bonding processing. In the presence of a mechanical driving force, crack/fractures can form on the films and grow over time.[13,14] These fracture-related behaviors have attracted considerable attention and have been studied with nanoindentation.[15,16] When a sharp tip (such as Vickers, Berkovich, or a cube-corner diamond tip) is indented into brittle materials, surface cracks often nucleate due to remnant "plastic" deformation and propagate outward from the tip in the radial direction. Since indentation behavior is coupled with the complex stress field arising from finite deformation, this behavior is implicitly related to the film's elastoplastic characteristics and fracture behavior.

In this work, we extend our previous work to explore the effect of water uptake on the fracture behavior of low-*k* porous OSG by analyzing the water-dependent film cracking threshold, crack morphology, and fracture toughness under stress corrosion using nanoindentation. We also search for potential processing methods to decrease the level of water-dependent changes to fracture properties.

For the purpose of examining how water uptake affects fracture behavior of low-*k* porous OSG, plasma-enhanced chemical-vapor-deposited (PECVD) SiCOH was used. The films were pretreated with Ar/O_2 plasma for demethylation/hypomethylation and to increase the number of hydrophilic groups in the low-*k* films.[17] After exposure to a humid ambient, several annealing temperatures and procedures were chosen so as to dehydrate separate water components out of these hydrophilic samples. Fourier-transform infrared spectroscopy (FTIR) was used to monitor the effectiveness of the dehydration, as well as any measurable chemical–structure change or damage that might be induced by annealing. High-load nanoindentation testing was carried out on a number of dehydrated films, in order to characterize the effect of in-diffused water on film-crack formation beneath the nanoindenter probe. To identify the influence of the various water components, the same measurements were repeated after conditioning the films under sequentially increased humidity, so that the amount of reabsorbed water by the hydrophilic groups in the annealed samples can be controlled. In addition, samples processed by ultraviolet (UV) curing, which is widely used to improve the mechanical properties of SiCOH,[18] were investigated to determine the effects of UV curing on the water-dependent fracture behavior of SiCOH thin films.

II. EXPERIMENT

Using our previously reported procedures,[11] experiments were performed on low-*k* porous SiCOH films with a *k*-value of 2.55, which were deposited on ⟨100⟩ *p*-type silicon substrates using PECVD and an organosilane precursor. The as-deposited thickness was 644 nm. In addition, for comparison, UV-cured SiCOH films using a Novellus SOLA Ultraviolet Thermal Processing system were also investigated. The film thickness after UV curing was measured using an ellipsometer to be 500 nm.

To ensure comparison with previous work, the SiCOH films were exposed to a humid environment for water uptake after being pretreated by plasma exposure, which was done for demethylation/hypomethylation and to increase the number of hydrophilic groups (mainly, hydroxyl groups, -OH). The humidity exposure was done by exposing the samples to high moisture content air [about 80% relative humidity (RH)] at room temperature for 60 h. The exposure time was chosen based on the moisture absorption and desorption dynamics model of *Yao et al.*,[19] to make sure the hydrophilic SiCOH film was water-saturated. Then, the hydrogen-bonded (α- or β-bonded) water absorbed by the films was removed selectively by setting different annealing temperatures using a programmable annealing system (190 °C annealing to remove α-bonded water and 400 °C annealing to remove β-bonded water) as described previously.[11] The annealing was carried on in a very mild condition by utilizing a low temperature-ramp rate and an equally low cooling-down speed, to avoid film delamination and to enable stress releasing. Both as-deposited and UV-cured SiCOH were treated under the same annealing conditions.

To monitor the effectiveness of the dehydration, and to characterize the residual stress that might be induced by annealing in the film or film/substrate interface, FTIR operated in the transmission mode was conducted on both nonannealed and annealed samples. The -OH relative absorbance peaks in PECVD SiCOH low-k films can be summarized as: O-H stretching (3300–3600 cm^{-1}), that is, H-bonded H_2O; stretching modes of isolated and terminal –OH(3650–3800 cm^{-1}); hydroxyl terminals (3690 cm^{-1}); isolated surface silanols Si-OH (3750 cm^{-1}); and Si-OH stretching (3200–3650 cm^{-1}).[20] By tracking and comparing these -OH related peaks, the effectiveness of dehydration can be monitored, as is shown in Fig. 1. These results are similar to the work of Kubasch[21] and were also verified in our previous work,[11] indicating that the absorbed water components (α- and β-bonded) can be effectively removed by annealing.

The FTIR absorption spectrum also provides information on the residual stress in the films. For these hybrid silica-based porous low-k dielectrics, the basic structural unit is an SiO_4-like tetrahedron.[18] The angle of the O-Si-O bonds is fixed at 109.5°; however, the Si-O-Si angle is rather flexible and is twofold coordinated since each O atom bridges two neighboring SiO_4 tetrahedrons. This bond is relatively easy to bend, stretch, or rotate.[22] Deconvolution analysis of the FTIR absorption spectrum assigned to the Si-O-Si skeleton, usually from 950 cm^{-1} to 1200 cm^{-1}, gives some insights of the states of different types of Si–O–Si bonds: Si-O-Si network ($\sim$1063 cm^{-1}), Si-O-Si cage ($\sim$1130 cm^{-1}), and Si-O-Si suboxide ($\sim$1023 cm^{-1}).[19] The bond strength of the Si-O-Si bonds is severely weakened when the bond angle deviates from the mean value of 144°.[23] The annealing-induced residual stress, if any, can be produced by the different fractions of the networked structure, the cage structure and the suboxide structure. Higher interfacial stress

Redistribution subject to AVS license or copyright; see http://scitation.aip.org/termsconditions. Download to IP: 128.104.180.203 On: Mon, 21 Apr 2014 19:50:41

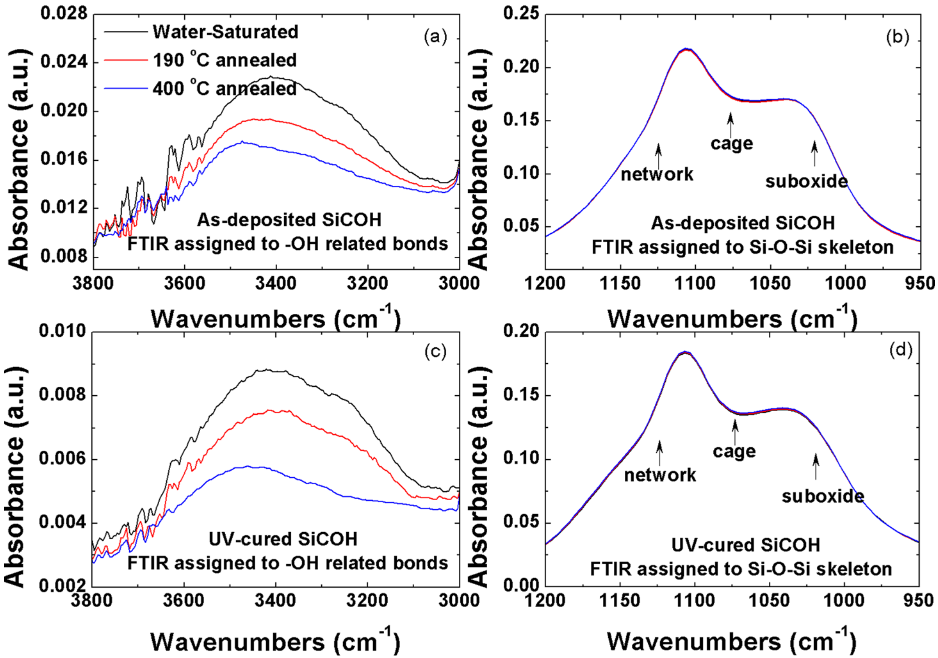

FIG. 1. (Color online) FTIR spectrum of the water-saturated, 190 °C annealed, and 400 °C annealed SiCOH films: (a) FTIR peaks assigned to -OH related bonds in as-deposited SiCOH; (b) FTIR peaks assigned to Si-O-Si skeleton in as-deposited SiCOH; (c) FTIR peaks assigned to -OH related bonds in UV-cured SiCOH; (d) FTIR peaks assigned to Si-O-Si skeleton in UV-cured SiCOH. Reprinted with permission from Guo *et al.*, J. Appl. Phys. **114**, 084103 (2013). Copyright 2013, American Institute of Physics.

is associated with a denser oxide film, a smaller Si–O–Si bond angle and a lower peak.[24] Thus, through the positions and amplitude of absorption frequency peaks of different types of Si–O–Si bonds (network, cage, or suboxide), the residual stress can be monitored. The FTIR spectra, for both nonannealed and annealed samples, as depicted in Fig. 1(b) for as deposited SiCOH and in Fig. 1(d) for UV cured SiCOH, showed no observable changes on the Si-O-Si related peaks after 190 °C/400 °C annealing.[11] The annealing-induced residual stress in the films is negligible.

In addition, the other main FTIR peaks from PECVD SiCOH remain almost unchanged after annealing.[11] The only variation in the SiCOH film characteristics induced by annealing is that due to the water components, and therefore, any fracture property changes should be water related.

The water-dependent fracture behavior of SiCOH films was investigated with a Hysitron TriboIndenter® equipped with a humidity-controllable enclosure, inside which the RH was controlled with an InstruQuest HumiSys™ HF relative humidity generator, enabling *in-situ* nanoindentation measurement on the samples under different humidities. Nanoindentation was first performed at 10% RH, followed by 38% and 73% RH at room temperature. The films were conditioned for a minimum of 24 h at each RH before testing. The experimental procedures are similar with previous work, and more details are available in Ref. 11.

A Zeiss LEO 1530 field emission scanning electron microscope (SEM) was used to image all residual indents. A very thin Au layer (∼60 nm) was sputter-coated on each specimen for high-quality SEM imaging. During the indentation process, if the load was sufficiently high, a crack was initiated from the indent corners. The crack propagates along the direction of the "contact radius"[25] and becomes longer and wider in the vicinity of the indents as P_{max} increases continuously, which we have shown previously.[11]

In this work, for each loading series, the threshold P_{max} of the indent at which the film crack was first observed was recorded. For each cracked indent, the fracture length, defined as the distance from the indent corner to crack tip, was measured. The profiles of the cracked indents were also analyzed and compared morphologically. We shall show that both the fracture length and the cracked-indent profiles are all related to the level of water uptake in these low-*k* films.

III. RESULTS AND DISCUSSION

A. Cracking threshold

First, a material-specific cracking threshold for SiCOH film is defined, followed by analysis showing how the water uptake in SiCOH can affect the film-cracking threshold during indentation.

In many works,[15,26] the cracking threshold is usually characterized by the maximum indentation load ($P_{\max}$). An attractive feature of using this method in nanoindentation is that the cracking-threshold load can be directly determined from the analysis of the load-depth trace. The implementation of this method is relatively straightforward. As illustrated in Fig. 2, $P_{\max}$ directly corresponds to the load-depth discontinuity point, which is often referred to as a "pop-in" event, as seen in the loading segment of the SiCOH load-depth trace. However, a significant problem exists in that the threshold $P_{\max}$ depends on the film thickness, generally being higher for films that have higher thicknesses. Since the SiCOH thickness changes after annealing dehydration and humidity

Redistribution subject to AVS license or copyright; see http://scitation.aip.org/termsconditions. Download to IP: 128.104.180.203 On: Mon, 21 Apr 2014 19:50:41

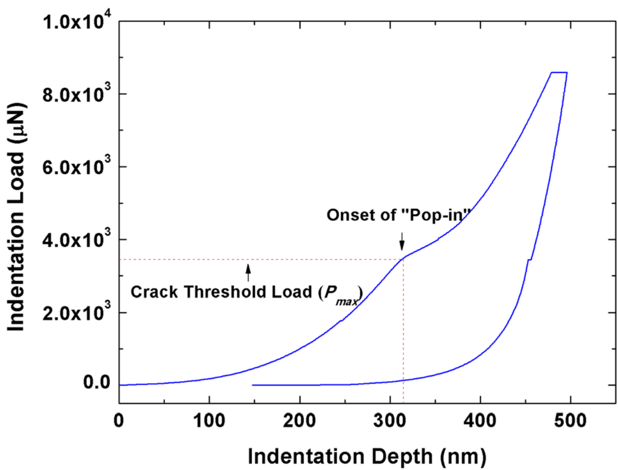

FIG. 2. (Color online) Representative pop-in identified in the loading segment of the SiCOH load-depth trace. The data comes from test on a 500 nm water-saturated UV-cured SiCOH film after conditioning at 10% RH. Reprinted with permission from Guo *et al.*, J. Appl. Phys. **114**, 084103 (2013). Copyright 2013, American Institute of Physics.

conditioning, determination of the cracking threshold in terms of P_{max} is not suitable to be used here.

Instead, there is another convenient, experimentally measureable parameter that can be used to identify the cracking threshold of given films with different thicknesses. The parameter is the indent size relative to the film thickness, i.e., the ratio of square root of the projected contact area of the indenter with the sample surface (A_c) to the film thickness (h_f). The load and depth of the loading segment "pop-in" in the load-depth trace corresponds, coincidentally, to the discontinuity point in the film hardness (H) versus $\sqrt{A_c}/h_f$ curve as shown in Fig. 3, where a decrease in film hardness is observed when the maximum loadings are above the cracking threshold P_{max}.

Figure 4 shows the effects of annealing dehydration and RH conditioning on the film-cracking thresholds, as a function

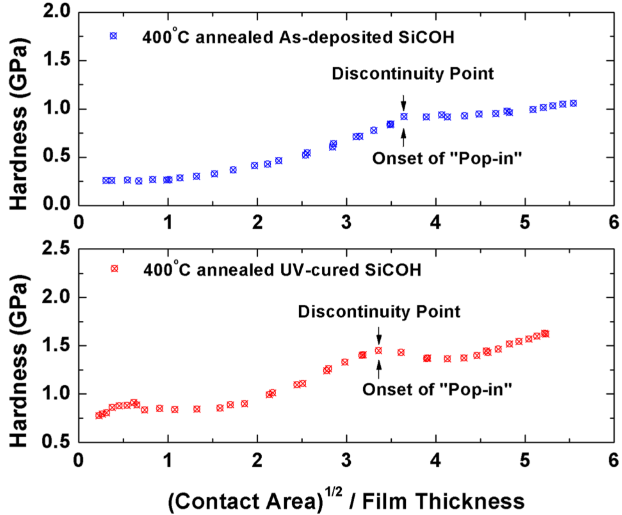

FIG. 3. (Color online) Hardness (H) of SiCOH films as a function of $\sqrt{A_c}/h_f$, where A_c is the contact area and h_f is the film thickness. The data comes from measurements on 400 °C annealed as-deposited and UV-cured SiCOH after conditioning at 10% RH. Reprinted with permission from Guo *et al.*, J. Appl. Phys. **114**, 084103 (2013). Copyright 2013, American Institute of Physics.

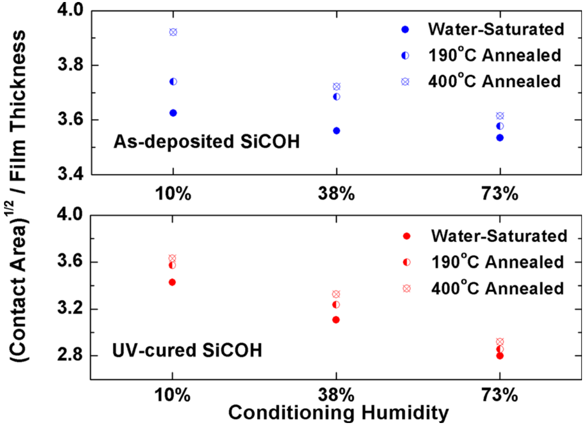

FIG. 4. (Color online) Film-crack thresholds evaluated by the indent size [i.e., square root of contact area normalized with respect to film thickness ($\sqrt{A_c}/h_f$)].

of the indent size—(square root of contact area normalized to film thickness) ($\sqrt{A_c}/h_f$). Higher values for the threshold value of $\sqrt{A_c}/h_f$ are defined to correspond to improved performance of the film. For the annealed dehydrated films, an increased threshold indent size for the film cracks compared with those for the water-saturated films was observed. Taking as-deposited SiCOH after 10% RH conditioning as an example, the film-cracking threshold values of $\sqrt{A_c}/h_f$ for (1) water-saturated, (2) α-bonded water removed, and (3) both α- and β-bonded water removed samples are 3.62, 3.74, and 3.92, respectively. The removal of α- or/and β-bonded water enhances the film's tolerance to stress corrosion, evaluated in terms of $\sqrt{A_c}/h_f$, by 3.3% and 8.3%, respectively. It should be noted that as $\sqrt{A_c}/h_f$ increases, the indentation load increases exponentially rather than linearly, as shown in Fig. 5. Thus, a small increase in $\sqrt{A_c}/h_f$ corresponds to a considerable increase of the indentation load. Evaluating the enhancement of the cracking threshold in terms of indentation load, according to Fig. 5, the removal of β-bonded water (400 °C annealing)

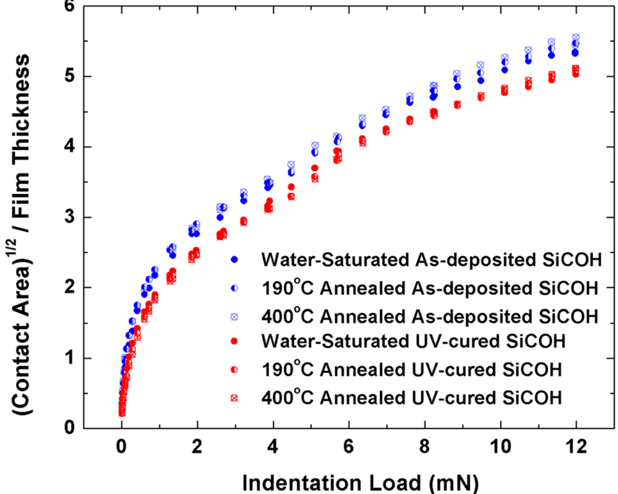

FIG. 5. (Color online) Correspondence between indentation load (P_{max}) and square root of the contact area normalized to film thickness ($\sqrt{A_c}/h_f$). The data comes from the measurements on water-saturated/annealed as-deposited and UV-cured SiCOH after conditioning at 10% RH.

Redistribution subject to AVS license or copyright; see http://scitation.aip.org/termsconditions. Download to IP: 128.104.180.203 On: Mon, 21 Apr 2014 19:50:41

increases the cracking threshold P_{max} by 0.62 mN. Comparing this with the cracking threshold P_{max} of the water-saturated sample (∼4.48 ± 0.02 mN), the increase is significant. These increases are likely attributed to decreased amounts of water in the films, which should, in fact, increase the cohesive fracture energy of the films.[27]

For all films, the threshold for film cracking decreases after conditioning at higher RH. For dehydrated (190 °C/400 °C) SiCOH films, there is a significant decrease of the cracking threshold after high RH conditioning, as shown in Fig. 4, indicating that the increase in the cracking threshold level induced by dehydration is offset by reabsorption of water during conditioning at higher RH. After conditioning at 73% RH, the cracking threshold of the annealed samples is almost the same as that for the water-saturated sample, indicating that the water-dependent increase in the cracking threshold associated with dehydration is reversible under these annealing conditions. Even for water-saturated samples, the cracking threshold decreases slightly after conditioning at higher RH. This will be explained subsequently.

Postprocessing UV curing is an important treatment for strengthening porous low-k dielectrics that improves their chemical stability and mechanical properties and is widely used during fabrication. Since both water solubility and diffusivity change due to UV-curing-induced structural rearrangements, the moisture intrusion and retention behavior is believed to be different from that of as-deposited samples.[19] Thus, it is also useful to determine the effects of UV curing on water-dependent film cracking thresholds. As depicted in Fig. 4, for annealing dehydration and RH conditioning, the film-cracking threshold for UV-cured SiCOH follows a similar trend to that of as-deposited SiCOH, i.e., (1) removal of α- and/or β-bonded water enhances the film's tolerance to stress corrosion and (2) RH conditioning counteracts the effects of annealing. However, the effects of annealing on UV-cured samples were weaker, accompanied by a smaller change in the cracking threshold *after* conditioning at higher RH. This smaller change in the cracking threshold can be attributed to the fact that the weak hydrophilic terminal bonds of Si-OH in the film under UV curing can be severed and replaced with hydrophobic cross-linked Si-O-Si bonds.[28] The decrease in the concentration of hydrophilic bonds (-Si-OH) lowers the equilibrium water content in the films, and as a result, no significant changes in the cracking threshold levels were seen after annealing. On the other hand, conditioning samples at *higher* RH significantly decreases the cracking-threshold level in UV-cured SiCOH.

This is believed to be attributed to the degradation of film adhesion energy induced by lateral water diffusion along the SiCOH/Si interface as follows. Isotope diffusion experiments by Li (Ref. 26) indicate that at room temperature, water diffuses mainly along the SiCOH/substrate interface and not through the porous films. This lateral water diffusion causes significant degradation of the film adhesion energy, while not changing the fracture energy of SiCOH very much. For dehydrated as-deposited SiCOH, the high degree of hydrophilicity of the SiCOH film partially lowers this preference for water diffusion, so only a small decrease of the cracking threshold after conditioning at higher RH was seen. However, for UV-cured SiCOH, the film/substrate interface is the main path for water diffusion. This shows that for UV-cured SiCOH, annealing dehydration does not affect the film-crack threshold significantly, while higher RH conditioning will significantly decrease the crack-threshold level.

B. Crack morphology

Above the cracking threshold, when gradually increasing the stress in a film attached to a substrate, the film will fail by the formation of a number of cracks propagating from the surface, through the dielectric and down to the interface and subsequent channeling across the film.[15] Analysis of these crack mechanics effectively reveals the material's elasto-plastic properties.[29] Here, the effect of water uptake on crack morphology of the indents can be determined.

Figure 6 shows SEM pictures of the cracked imprints on the water-saturated, 190 °C and 400 °C annealed as-deposited SiCOH films after conditioning at gradually increasing humidity. It appears that surface cracks are the desired configurations for radical cracks, because one end of the crack is pinned at the corner of the impression, and due to the presence of the indenter, this end cannot propagate inward. In addition, only the far end grows outward radially, i.e., it emanates from the indent corners.[15] It is necessary to point out that for all of the indents shown here, the indent size relative to the film thickness ($\sqrt{A_c}/h_f$) is the same. Thus, the observed differences of the crack morphology of the residual indents, if any, should reflect the effects of water uptake on the films crack morphology.

Figure 6(a) shows the cracked indents on, from left to right, water-saturated, 190 °C and 400 °C annealed SiCOH films after conditioning at 10% RH. It is seen that both the crack length and crack-opening displacements decrease with reduced water in the film, indicating annealing dehydration increases the ductility of SiCOH films compared with the water-saturated samples, which are therefore shown to be more fragile. In addition, the cracks on the 190 °C and 400 °C annealed SiCOH films are somewhat asymmetric. This is likely due to the increased resistance to cracks propagating through the film. This is consistent with the changes in the crack threshold in Sec. III A, which we have shown to be enhanced by dehydration after annealing.

After conditioning at higher RH, the profiles of the cracks in the water-saturated, 190 °C and 400 °C annealed dehydrated samples are nearly identical, as shown in Figs. 7(b) and 7(c). Figure 7 shows the SEM images of the residual indents induced by the same indent size ($\sqrt{A_c}/h_f$), for the water-saturated, 190 °C and 400 °C annealed UV-cured SiCOH films after conditioning at 10% RH. Again, this shows that annealing dehydration enhances the film resistance to both crack occurrence and propagation.

C. Fracture toughness

Fracture toughness, which is defined as the measure of material resistance to extension of a crack, plays a critical role in applications of different engineering components and

Redistribution subject to AVS license or copyright; see http://scitation.aip.org/termsconditions. Download to IP: 128.104.180.203 On: Mon, 21 Apr 2014 19:50:41

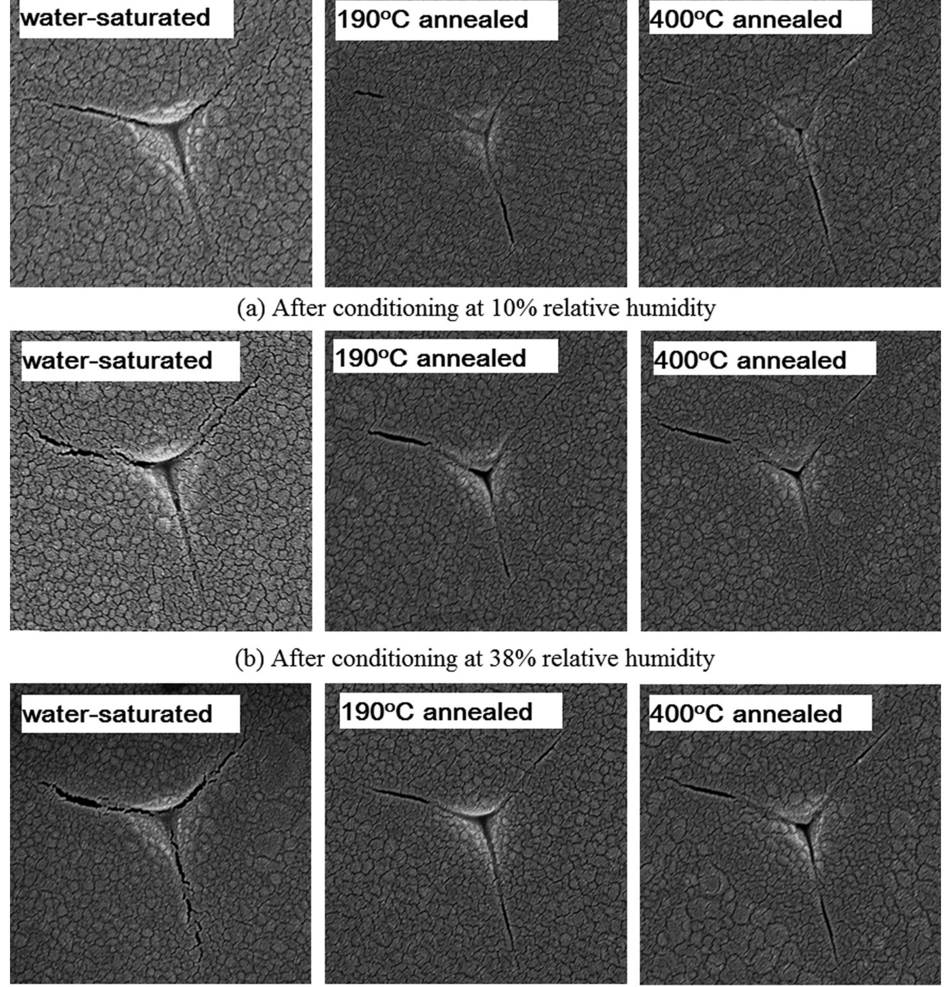

FIG. 6. SEM-imaged crack morphology of the residual imprints for as-deposited SiCOH films, after conditioning at gradually increased humidity with same indent sizes: (a) relative humidity of 10%; (b) relative humidity of 38%; and (c) relative humidity of 73%.

structures, e.g., structural-integrity assessment, damage-tolerance design, and residual stress analysis.[30] In this section, measurement of the fracture toughness of the SiCOH films and how it is affected by water uptake was undertaken.

The most widely used analysis in the literature[25,31] for assessing the fracture toughness of a sharp tip indent crack utilizes the expression

$$K_c = \alpha \left(\frac{E}{H}\right)^{1/2} \left(\frac{P_{\max}}{c^{3/2}}\right), \quad (1)$$

where K_c is the fracture toughness, E is the elastic modulus, H is the hardness, $P_{\max}$ is the maximum loading, and c is the length of the surface trace of the crack measured from the center of the indent. Here, α is an empirical calibration

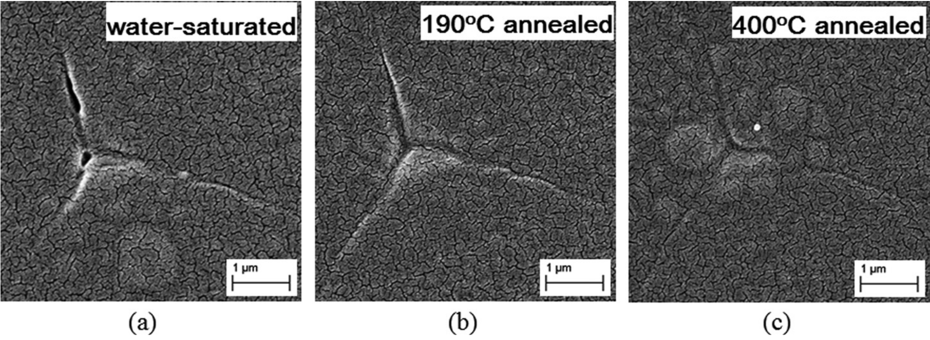

FIG. 7. SEM-imaged crack morphology of the residual imprints for UV-cured SiCOH films, after conditioning at relative humidity of 10% with same indent sizes: (a) water-saturated; (b) 190 °C annealing dehydrated; and (c) 400 °C annealing dehydrated.

Redistribution subject to AVS license or copyright; see http://scitation.aip.org/termsconditions. Download to IP: 128.104.180.203 On: Mon, 21 Apr 2014 19:50:41

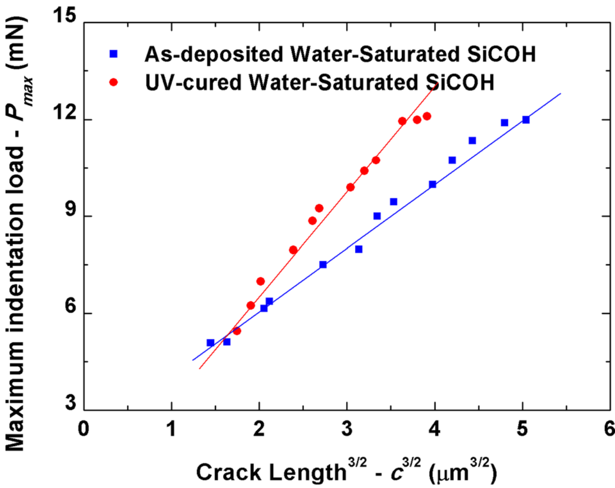

FIG. 8. (Color online) 3/2 power of film crack length (c) as a function of the maximum indentation load (P_{max}). The data comes from water-saturated as-deposited and UV-cured SiCOH after conditioning at 10% RH.

constant that depends on the geometry of the indenter. In many cases, the calibration constant is not derived from physical models and is arrived at by curve-fitting. Typically, α is usually taken to be 0.016 ± 0.004 based on a fit to experimental data using independent fracture-toughness measurements.[32] However, the standard deviation of the fit needed to obtain the calibration constant is large ($\pm 25\%$). The toughness determined using Eq. (1) is only within $\pm 50\%$ of the actual value at the 95% confident interval. In addition, in the case of thin-film radial fractures, because of perturbation by the substrate, film densification, and residual stresses in the film, quantifying the fracture toughness accurately becomes more complicated.

Volinsky[31] demonstrated a nearly linear relationship between the maximum indentation load (P_{max}) and the crack length (c) to the 3/2 power, and estimated low-k dielectric film fracture toughness to range from 0.01 to 0.05 $\mathrm{MPa}\cdot\sqrt{\mathrm{m}}$. To determine the effects of water uptake on film fracture toughness, the crack length (c) to the 3/2 power as a function of the maximum indentation load (P_{max}) is also plotted, for which $c^{3/2}$ versus P_{max} shows a roughly linear relationship similar to the results of Volinsky,[31] as depicted in Fig. 8. Since the geometry of all of the pyramid indenter tips used in the experiment is identical, the influence from the uncertainty of the calibration constant (α) to the measured toughness can be ignored and Eq. (1) can be simplified to Eq. (2).The water-dependent elastic modulus (E) and hardness (H) for SiCOH have been determined previously.[11] Extrapolating a linear fit to the P_{max} versus $c^{3/2}$ curve yields a ranking of the relative toughness of water-saturated and annealed SiCOH using

$$K_c \approx \text{const} * \left(\frac{E}{H}\right)^{1/2} \left(\frac{P_{max}}{c^{3/2}}\right). \tag{2}$$

Using Eq. (2), we estimate 0.03 $\mathrm{MPa}\cdot\sqrt{\mathrm{m}}$ to be the median of the reported low-k dielectric film fracture toughness range (0.01–0.05 $\mathrm{MPa}\cdot\sqrt{\mathrm{m}}$)[30] as the fracture toughness for the water-saturated as-deposited SiCOH films after conditioning at 10% RH. Table I summarizes the relative percentage changes of the fracture toughness for all SiCOH film, based on the results for 10% RH conditioned water-saturated film. As seen, dehydration causes a very small decrease in the film-fracture toughness for as-deposited SiCOH. For example, after 10% RH conditioning, the 400 °C annealed sample, from which both α- and β-bonded water were removed, has a 2.7% decrease in toughness compared with the water-saturated sample. For the 190 °C annealed sample, the toughness decreased by 1.6%, which can be ignored considering the $\pm 50\%$ error for the toughness measurements. On the other hand, after conditioning at high RH, for both water-saturated samples and annealed dehydrated samples, the toughness remained almost the same, demonstrating that water uptake from the ambient humidity has a negligible effect on the fracture toughness for as-deposited nanoporous low-k SiCOH films. This has been validated by examining the variation of the elastic modulus and hardness with annealing dehydration and RH conditioning in previous work.[11] In that work, it was shown that the film elastic modulus decreases and the film hardness increases after annealing. Thus, after annealing dehydration, the decrease in the value of $(E/H)^{1/2}$, the second term in Eq. (2), will counteract the increase in $P_{max}/c^{3/2}$, the third term in Eq. (2). This synergy decreases the effect of in-diffused water on the film toughness.

For UV-cured SiCOH, because of the higher value of $P_{max}/c^{3/2}$ shown in Fig. 8, the water-saturated SiCOH

TABLE I. Measured fracture toughness for SiCOH films with different annealing dehydration and humidity conditioning. The percentage increase or decrease in the fracture toughness was calculated based on the result of water-saturated sample after conditioning at 10% RH. The percentage increase/decrease was calculated based on the results of water-saturated sample after conditioning at relative humidity of 10%. "-" represents no change or negligible change; "↗/↘" means mild increases/decreases; and "↑/↓" means significant increases/decreases.

Dielectric films under different RH conditioning		Fracture toughness ($\mathrm{MPa}\cdot\sqrt{\mathrm{m}}$) 10%	38%	73%
As-deposited	Water-saturated	0.30 (-)	0.9% (↘)	1.0% (↘)
	190 °C annealed	1.6% (↘)	1.7% (↘)	1.5% (↘)
	400 °C annealed	2.7% (↘)	2.5% (↘)	2.1% (↘)
UV-cured	Water-saturated	0.50 (-)	0.8% (↗)	2.1% (↗)
	190 °C annealed	11.6% (↑)	9.6% (↑)	2.2% (↗)
	400 °C annealed	16.3% (↑)	12.1% (↑)	3.4% (↗)

Redistribution subject to AVS license or copyright; see http://scitation.aip.org/termsconditions. Download to IP: 128.104.180.203 On: Mon, 21 Apr 2014 19:50:41

fracture toughness was estimated to be $0.05\,\text{MPa}\cdot\sqrt{\text{m}}$. The relative percentage changes of film fracture toughness for a number of dehydrated samples are also summarized in Table I. Unlike as-deposited SiCOH, dehydration causes the film fracture toughness of UV-cured SiCOH to increase as compared with water-saturated samples. As shown in Table I, 400 °C annealing increases the film toughness by 16.3%, and for 190 °C annealing, the increase is 11.6%. This is the case because, for UV-cured SiCOH, the film elastic modulus (E) can be enhanced after annealing dehydration. Thus, the increased $P_{\max}/c^{3/2}$, combined with increased elastic modulus (E) by annealing, yields the increased film fracture toughness of UV-cured SiCOH.

IV. CONCLUSION

In this work, the effects of in-diffused water on the fracture behavior of low-k porous organosilicate glass (SiCOH) were examined using nanoindentation. The roles of physisorbed (α-bonded) and chemisorbed (β-bonded) water were examined separately by conditioning the annealed samples under sequentially increased humidity. Nanoindentation results showed that either the loading segment pop-in in the load-depth trace, the discontinuity in the H versus $\sqrt{A_c}/h_f$ curve, or direct observation using SEM imaging can be used to identify the threshold $P_{\max}$ for film fracture during nanoindentation loading. The cracking threshold, crack morphologies, and fracture toughness for the low-k porous films are all implicitly related to water uptake in the materials. We thus conclude that, for as-deposited SiCOH, annealing dehydration enhances the elastoplastic properties of SiCOH films and increases their resistance to cracking, but has negligible effect on the film–fracture toughness. For UV-cured SiCOH, annealing dehydration can increase the film–fracture toughness while retaining its smaller effect on the film elastoplastic properties.

The mechanical properties of low-k films must be optimized for improved elastoplastic characteristics and fracture resistance. This fundamental understanding of the influence of water uptake on film–fracture behavior supports the necessity to inhibit water uptake during fabrication and post-processing, and proposes this as a method to enhance film fracture resistance.

ACKNOWLEDGMENTS

This work was supported by the Semiconductor Research Corporation under Contract No. 2012-KJ-2359, by the National Science Foundation under Grant CBET-1066231 and by the Applied Materials University Research Partnership Program. J. E. Jakes is supported by USDA Forest Service PECASE funding.

[1] K. Maex, M. R. Baklanov, D. Shamiryan, F. Iacopi, S. H. Brongersma, and Z. S. Yanovitskaya, J. Appl. Phys. **93**, 8793 (2003).
[2] M. R. Baklanov and K. Maex, Philos. Trans. Roy. Soc. A **364**, 201 (2006).
[3] A. Grill, J. Appl. Phys. **93**, 1785 (2003).
[4] D. Shamiryan, M. R. Baklanov, S. Vanhaelemeersch, and K. Maex, J. Vac. Sci. Technol. B **20**, 1923 (2002).
[5] M. R. Baklanov, K. P. Mogilnikov, and Q. T. Le, Microelectron. Eng. **83**, 2287 (2006).
[6] H. Shi, J. Bao, R. S. Smith, H. Huang, J. Liu, P. S. Ho, M. L. McSwiney, M. Moinpour, and G. M. Kloster, Appl. Phys. Lett. **93**, 192909 (2008).
[7] J. Shoeb and M. J. Kushner, J. Vac. Sci. Technol. A **30**, 041304 (2012).
[8] Y. Li, I. Ciofi, L. Carbonell, N. Heylen, J. V. Aelst, M. R. Baklanov, G. Groeseneken, K. Maex, and Z. Tokei, J. Appl. Phys. **104**, 034113 (2008).
[9] J. R. Lloyd, T. M. Shaw, and E. G. Liniger, *Proceedings of the IEEE International Integrated Release Workshop Final Report* (2005), p. 39.
[10] L. Broussous, G. Berthout, D. Rebiscoul, V. Rouessac, and A. Ayral, Microelectron. Eng. **87**, 466 (2010).
[11] X. Guo, J. E. Jakes, M. T. Nichols, S. Banna, Y. Nishi, and J. L. Shohet, J. Appl. Phys. **114**, 084103 (2013).
[12] J. Proost, E. Kondoh, G. Vereecke, M. Heyns, and K. Maex, J. Vac. Sci. Technol. B **16**, 2091 (1998).
[13] T. Y. Tsui, A. J. McKerrow, and J. J. Vlassak, J. Mech. Phys. Solids **54**, 887 (2006).
[14] E. P. Guyer, M. Patz, and R. H. Dauskardt, J. Mater. Res. **21**, 882 (2006).
[15] G. M. Pharr, Mater. Sci. Eng. A-Struct. **253**, 151 (1998).
[16] J. J. Vlassak, M. D. Drory, and W. D. Nix, J. Mater. Res. **12**, 1900 (1997).
[17] J. Shoeb, M. M. Wang, and M. J. Kushner, J. Vac. Sci. Technol. A **30**, 041303 (2012).
[18] N. Kemeling, K. Matsushita, N. Tsuji, K. Kagami, M. Kato, S. Kaneko, H. Sprey, D. Roest, and N. Kobayashi, Microelectron. Eng. **84**, 2575 (2007).
[19] J. Yao, A. Iqbal, H. Juneja, and F. Shadman, J. Electrochem. Soc. **154**, G199 (2007).
[20] M. R. Baklanov, J. D. Marneffe, D. Shamiyan, A. M. Urbanowicz, H. Shi, T. V. Rakhimova, H. Huang, and P. S. Ho, J. Appl. Phys. **113**, 041101 (2013).
[21] C. Kubasch, H. Schumacher, H. Ruelke, U. Mayer, and J. W. Bartha, IEEE Trans. Electron Devices **58**, 2888 (2011).
[22] T. Yang and K. C. Saraswa, IEEE Trans. Electron Dev. **47**, 746 (2000).
[23] J. T. Fitch, C. H. Bjorkman, and G. Lucovsky, J. Vac. Sci. Technol. B **7**, 775 (1989).
[24] G. Lucovsky, M. J. Manitini, J. K. Srivastava, and E. A. Irene, J. Vac. Sci. Technol. B **5**, 530 (1987).
[25] Y. Tang, A. Yonezu, N. Ogasawara, N. Chiba, and X. Chen, Proc. R. Soc. Lond., Ser. A **464**, 2967 (2008).
[26] D. S. Harding, W. C. Oliver, and G. M. Pharr, Mater. Res. Soc. Symp. Proc. **356**, 663 (1994).
[27] H. Li, T. Y. Tsui, and J. J. Vlassak, J. Appl. Phys. **106**, 033503 (2009).
[28] F. Iacopi *et al.*, J. Appl. Phys. **99**, 053511 (2006).
[29] C. A. Schuh, Mater. Today **9**, 32 (2006).
[30] X. Zhu and J. A. Joyce, Eng. Fract. Mech. **85**, 1 (2012).
[31] A. A. Volinsky, J. B. Vella, and W. W. Gerberich, Thin Solid Films **429**, 201 (2003).
[32] G. R. Anstis, P. Chantikul, B. R. Lawn, and D. B. Marshall, J. Am. Ceram. Soc. **64**, 533 (1981).

Redistribution subject to AVS license or copyright; see http://scitation.aip.org/termsconditions. Download to IP: 128.104.180.203 On: Mon, 21 Apr 2014 19:50:41